Proceedings of the 10th World Congress on Mechanical, Chemical, and Material Engineering (MCM'24)
Barcelona, Spain - August 22-24, 2024
Paper No. ICMIE 161
DOI: 10.11159/icmie24.161

Dynamic Analysis of Fluid-Filled Ring-Stiffened Conical Shells

A. A. Lakis[1], M. A. Esmaeilzadehazimi[2], M. Toorani[2]
[1] Mechanical Engineering Department, Ecole Polytechnique of Montreal
Montreal, Quebec, Canada
Aouni.lakis@polymtl.ca; mohammadamin.esmaeilzadehazimi@polymtl.ca
[2]Mechanical System Engineering, Conestoga College
Cambridge, Ontario, Canada
mtoorani@conestogac.on.ca

Abstract **-** This paper presents a mathematical model developed for the dynamic analysis of ring-stiffened conical shell subject to a flowing fluid. The proposed approach combines classical shell theory and the finite element method, making use of displacement functions derived from exact solutions of Sanders' shell equations. Mass and stiffness matrices are determined by precise analytical integration of the equations of motion. The analysis of the shell-fluid interface involves leveraging the velocity potential, Bernoulli's equation, and impermeability conditions to determine an explicit expression for fluid dynamic pressure. Three distinct force vectors induced by the fluid (called the inertial, centrifugal, and Coriolis forces) can be determined through analytical integration of fluid dynamic pressure over structural shape functions. The influence of physical and geometrical parameters on the fluid-structure system has been considered in the numerical solutions. This study explores the influence of geometric parameters, stiffener quantity, cone angle, and applied boundary conditions on the natural frequency and instability characteristics of fluid-loaded ring-stiffened conical shells. When these results are compared with corresponding ones available in the open literature, both theoretical and experimental, very good agreement is obtained.

Keywords**:** Stiffened Conical Shell, Flowing Fluid, Vibrations

1. Introduction

Shells are commonly used in various industries, including aerospace, civil engineering, and oil and petrochemical sectors, and understanding their dynamic behaviour when subjected to different loads is crucial for safe utilization. Conical shells have received less attention in research due to mathematical complexity. Ring-stiffeners are used for shell stiffening, and cylindrical shells with ring-stiffeners have received more attention than conical shells.

The vibration analysis of shell-type structures in the presence of stationary fluid is of great interest in aeronautical and mechanical engineering. Lakis et al. [1] introduced a theoretical approach that combines the finite element method with Sanders' shell theory to derive displacement functions for dynamic analysis of shells in a stationary fluid environment. Kerboua et al. [2] extended this method to predict the dynamic behaviour of anisotropic truncated conical shells containing fluid by introducing a damping term in the fluid-structure interaction equation. Rahmanian et al. [3 and 4] introduced a reduced-order formulation for vibration analysis of conical shells filled with quiescent fluid. They also investigated the dynamic response of conical and cylindrical shells carrying fluid, employing Flügge's shell theory.

Chen et al. [5] investigated the vibrational behaviour and far-field sound radiation of a submerged stiffened conical shell at low frequencies. A power series solution was employed to analyse the dynamic response of the shell, considering ring stiffeners modelled using a smeared approach. Liu et al. [6] proposed an analytical method to analyse the free vibration of external ring-stiffened conical shells with variable thickness under fluid loading. Banijamali and Jafari's [7] study focused on the free vibration of rotating conical shells with functionally graded materials and anisogrid reinforcement. The smeared method combined the shell and stiffeners' stiffness, considering material variations through thickness. The researchers evaluated how shell composition, stiffeners, rotation, and boundary conditions affect natural frequencies. Several recent studies also investigated the combined behaviour of stiffened and unstiffened conical-cylindrical shells [8-10]. Saboo and Kumar [11] examined a base-supported, partially filled fluid-shell system resembling a fast reactor's pressure vessel consisting of cylindrical and conical sections. Using Donnell's theory for shell characterization and a velocity potential model for the fluid, natural frequencies were deduced by minimizing an energy functional, with validation against analogous joined

systems. Zarei et al. [12] investigated vibration characteristics of composite conical shells reinforced with bevel stiffeners using experimental, analytical, and numerical methods, deriving governing equations with a shear deformation theory and the Ritz method, validated through experiments.

Prior research has extensively examined fluid-structure interaction in conical shells without considering the ring stiffeners and flowing fluid effects. There is a notable research gap in understanding the dynamic behaviour of ring-stiffened conical shells conveying fluid. To address this gap, Kumar and Ganesan's [13] work was extended using a finite element approach that combines Sanders' shell theory with finite element analysis. This investigation focuses on the response of truncated ring-stiffened conical shells subjected to the effects of flowing fluid. The proposed model utilizes a finite element approach that combines classical thin shell theory and finite element analysis, employing truncated cone two-node circular shells with four degrees of freedom per node. Displacement functions were derived from Sanders' shell equations. Linear potential flow theory was employed to effectively describe fluid-structure interaction due to small shell displacements. The velocity potential function, Bernoulli's equation, and an impermeability condition were used to determine pressure distribution, which led to the computation of three fluid forces exerted by the moving fluid on the structure's wall. The product of dynamic pressure and structural shape function was integrated across the fluid-structure interface to assess the inertial, centrifugal, and Coriolis forces induced by fluid loading. This comprehensive analysis considers the effect of geometrical and physical parameters of fluid and structures (e.g. flow velocity, boundary conditions, the number of rings, ring spacing, etc.) on the dynamic characteristics of the fluid-structure system.

2. Structural Modelling

Figure 1 shows the geometric features of a truncated conical shell. This shell has varying thickness, denoted as h, and is bounded by circular nodes i and j. The position along the x-axis is referred to as meridional coordinates. The small and large end radii are denoted as R_1 and R_2, with and x-direction length of L and a semi-vertex angle of α. The circumferential coordinate is denoted as θ. The finite element used to model the structure has four degrees of freedom at each node; one rotation $\frac{\partial W}{\partial x}$ and three displacement components (U, V, W) in axial, tangential, and radial direction, respectively. The displacement vector at node i is represented as δ_i as given below.

$$\{\delta_i\} = \left\{ U_i \; V_i \; \frac{\partial W_i}{\partial x} \; V_i \right\}^T \tag{1}$$

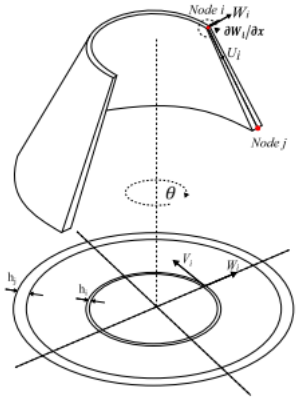

Fig. 1: Schematic of a conical shell and the corresponding degrees of freedom.

As shown in Figure 2, the height of the ring is added to the shell thickness at the top or bottom of the mid-plane for external and/or internal rings.

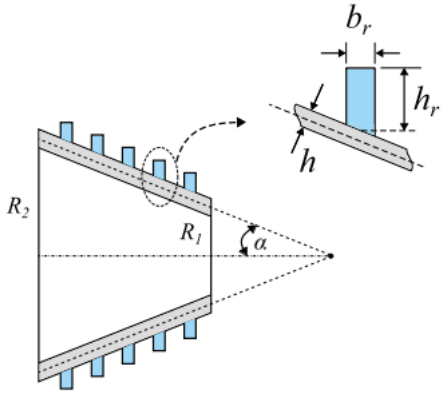

Fig. 2: Ring geometry.

2.1. Equations of Motion

The equations of motion for an anisotropic conical shell can be written as a function of displacement components, their derivatives, and material properties as:

$$L_k\left(U, V, W, P_{ij}\right) = 0; \qquad k = 1 \cdots 3 \;\&\; i, j = 1 \cdots 6 \tag{2}$$

The explicit form of the above equations is given in [14]. The P_{ij}, terms, constituting the material properties matrix $[P]_{6\times6}$ is given in [14]. The following displacement functions are used for the proposed model, where n is the circumferential mode number and $u_n, w_n, and\ v_n$ are the magnitudes of the displacements.

$$\{U(x,\theta)\ W(x,\theta)\ V(x,\theta)\ \} = \sum_{n=0}^{\infty}[T]\{u_n(x)\ w_n(x)\ v_n(x)\ \} =$$
$$\sum_{n=0}^{\infty}[cosn\theta\ 0\ 0\ 0\ cosn\theta\ 0\ 0\ 0\ sinn\theta\ ]\left(\frac{x}{l_e}\right)^{\frac{\lambda-1}{2}}\{\underline{A}\ \underline{B}\ \underline{C}\ \} \tag{3}$$

Where $\lambda, \underline{A}, \underline{B}, and\ \underline{C}$ are complex numbers and l_e is the length of the element. Substitution of equation (3) into equation (2) and conducting the intermediate mathematical manipulations result in the following characteristic equations:

$$h_8\lambda^8 + h_6\lambda^6 + h_4\lambda^4 + h_2\lambda^2 + h_o = 0 \tag{4}$$

Each complex root of equation (4) provides a solution to the system of equation (2). The complete solution is the sum of all eight roots. Using these equations, we could derive the following equation that describes the displacement functions in terms of the nodal displacement vector [14].

$$\{U(x,\theta)\ W(x,\theta)\ V(x,\theta)\ \} = [T][R][A]^{-1}\{\delta_i\ \delta_j\ \} = [N]\{\delta_i\ \delta_j\ \} \tag{5}$$

[N] is constituting the shape functions and matrices $[R]\ and\ [A]$ are given in [14].

2.2. Structural Mass and Stiffness Matrices

The mass and stiffness matrices for each element of a conical shell are given as:

$$[m_e] = \int \rho[N]^T[N]dV = \rho\int[A^{-1}]^T[R]^T[T]^T[T][R][A^{-1}]xsin(\alpha)hdxd\theta \tag{6}$$

$$[k_e] = \int [B]^T [P][B] dV = \int [A^{-1}]^T [Q]^T \left[[T]\ [0]\ [0]\ [T]\right]^T [P] \left[[T]\ [0]\ [0]\ [T]\right] [Q][A^{-1}] x sin(\alpha) h dx d\theta \quad (7)$$

Where ρ is the material density and [Q] is given in [14]. These integrals are calculated analytically to obtain the structural element mass and stiffness matrices. The global mass $[M_s]$ and stiffness $[K_s]$ matrices are formed by superimposing the element mass and stiffness matrices.

3. Fluid Modelling

Fluid pressure acting upon the structure is generally expressed as a function of out-of-plane displacement and its derivatives, i.e., velocity and acceleration. These three terms are respectively known as the centrifugal, Coriolis, and inertial forces. The fluid model is developed based on the following hypotheses: i) the fluid flow is a potential; ii) vibration is linear (small deformations); iii) the fluid mean velocity distribution is constant across the cross-section; iv) the fluid is incompressible; and v) the fluid is inviscid. Considering the assumptions, the velocity potential must satisfy the Laplace equation. This relation in the conical coordinate system is expressed as:

$$\nabla^2 \phi = \frac{2}{x}\frac{\partial \phi}{\partial x} + \frac{\partial^2 \phi}{\partial x^2} + \frac{1}{x^2 (sin\alpha)^2}\frac{\partial^2 \phi}{\partial \theta^2} + \frac{1}{x^2 tan\alpha}\frac{\partial \phi}{\partial \alpha} + \frac{1}{x^2}\frac{\partial^2 \phi}{\partial \alpha^2}. \quad (8)$$

Where ϕ is potential function. The fluid velocity components in $x, \theta, and\ \alpha$ directions in the conical coordinate system can be written as derivations of the potential function as follows:

$$V_x = \frac{Q}{x^2} + \frac{\partial \phi}{\partial x}, \quad V_\theta = \frac{1}{x sin\alpha}\frac{\partial \phi}{\partial \theta}, \quad V_\alpha = \frac{1}{x}\frac{\partial \phi}{\partial \alpha}, \quad (9)$$

where $V_x, V_\theta, and\ V_\alpha$ are the $x, \theta, and\ \alpha$ components of the fluid velocity and $\frac{Q}{x^2}$ is the unperturbed flow velocity along the shell in the x-direction. The remaining components in the above equation are perturbation fluid velocities in three directions. By employing Bernoulli's equation, the hydrodynamic pressure can be expressed in relation to the velocity potential as given below:

$$p = -\rho_f \left[\frac{\partial \phi}{\partial t} + \frac{Q}{x^2}\frac{\partial \phi}{\partial x}\right]_{\xi = a} \quad (10)$$

Where ρ_f represents the fluid density, ξ denotes the coordinate along the cone semi-vertex angle, and a represents the half-angle of the inner wall opening of the shell [14]. The impermeability condition ensures the permanent contact between the shell structure's surface and the peripheral fluid. This condition requires the vertical component of the fluid's velocity to be equivalent to the rate of change of the shell's radial displacement.

$$(V_\alpha)_{\alpha = a} = \frac{1}{x}\frac{\partial \phi}{\partial \alpha}|_{\alpha = a} = \left[\dot{W} + \frac{Q}{x^2} W'\right]_{\xi = a} \quad (11)$$

Where W is the radial displacement of the shell. The technique of separation of variables is adopted for solving the velocity potential.

$$\phi(x, \theta, \alpha, t) = \sum_{q=1}^{8} R_q(\alpha) S_q(x, \theta, t) \quad (12)$$

Where $R_q(\alpha)\ and\ S_q(x, \theta, t)$ are two separate functions to be defined, one can use equations (11 and 12) to develop the potential function as:

$$\phi(x,\theta,\alpha,t) = \sum_{q=1}^{8} x \frac{R_q(\alpha)}{R_q^{'}(\alpha)} \left[\dot{W} + \frac{Q}{x^2} W'\right]_{\alpha=a} \tag{13}$$

The only unknown function in equation (13) is $R_q(\alpha)$. By introducing equation (13) into equation (8), we obtain the following second-order differential equation:

$$R_q''(\alpha) + \frac{1}{tan\alpha} R_q'(\alpha) - \frac{n^2}{sin^2\alpha} R_q(\alpha) = 0 \tag{14}$$

In the case of internal flow, the truncated solution to differential equation (14) is given as:

$$R(\alpha) = C_1 cosh\left\{n\left[log\left(cos\left(\frac{\alpha}{2}\right)\right) - log\left(sin\left(\frac{\alpha}{2}\right)\right)\right]\right\} \tag{15}$$

Upon substitution of equations (13 and 15) into equation (10) and conducting some mathematical manipulation, one can derive the following equation to express the fluid dynamic pressure.

$$P_{int} = -\rho_f \left\{x[T]\left[R_{f1}\right][A]^{-1}\{\ddot{\delta}\} + \left(\frac{Q}{x^2}\right)[T]\left[R_{f2}\right][A]^{-1}\{\dot{\delta}\} + \left(\frac{Q^2}{4x^5}\right)[T]\left[R_{f3}\right][A]^{-1}\{\delta\}\right\} \tag{16}$$

Where $\left[R_{fi}\right] and\ [A]$ matrices are given in [14]. Integration of this dynamic pressure over the structural shape function results in finding the force vector induced by fluid as given below:

$$\begin{cases} \left[m_f\right] = -\rho_f \int x[N]^T[T]\left[R_{f1}\right][A]^{-1} x sin(\alpha) dx d\theta \\ \left[c_f\right] = -\rho_f Q \int \frac{1}{x^2}[N]^T[T]\left[R_{f2}\right][A]^{-1} x sin(\alpha) dx d\theta \\ \left[k_f\right] = -\frac{\rho_f Q^2}{4} \int \frac{1}{x^5}[N]^T[T]\left[R_{f3}\right][A]^{-1} x sin(\alpha) dx d\theta \end{cases} \tag{17}$$

These matrices represent the influence of inertial, Coriolis, and centrifugal effects. The Coriolis force arises due to an interaction between the relative velocity of the fluid and the rotation of the structural cross-section. These effects can result in both static (buckling) and dynamic (flutter) instabilities within the coupled fluid-structure system. The equation of motion for this coupled fluid-structure system is given as:

$$\left([M_s] + \left[M_f\right]\right)\{\ddot{\delta}_T\} + \left(\left[C_f\right]\right)\{\dot{\delta}_T\} + \left([K_s] + \left[K_f\right]\right)\{\delta_T\} = \{F\} \tag{18}$$

The state-space method is adopted to transform the system of equations into a set of 2n first-order differential equations where n represents the degrees of freedom. Therefore, the eigenvalue problem is given as:

$$|[DD] - \Lambda[I]| = 0 \tag{19}$$

Where [DD] is defined as:

$$[DD] = \left[[0]\ [I]\ -[M]^{-1}[K]\ -[M]^{-1}[C]\ \right] \tag{20}$$

Eigenvalue is expressed as a dimensionless parameter given below:

$$\Omega = \omega R_2 \sqrt{\rho(1-\nu^2)/E} \tag{21}$$

Where ω is natural frequency and R_2 is the large end radius of the shell.

3. Results and Discussions

In the first place, a convergence test was conducted to determine the required number of elements for dynamic analysis of both stiffened and unstiffened shells. A series of computations were conducted on a conical shell and the computed dimensionless frequencies were compared with experimental data available in [15]. Some results are given in Table 1 which indicates that the proposed model is achieving accuracy using fewer number of elements. Data used for this test are:

$$\alpha = 14.2^o, \rho = 7988\frac{kg}{m^3}, h = 0.254mm, R_1 = 0.0691m, R_2 = 0.1541m, E = 203GPa,$$
$$\nu = 0.3, and\ simply - supported\ boundary\ conditions.$$

Table 1: Dimensionless parameters of a conical shell in vacuo

Mode number	N_e=8	N_e=20	N_e=30	Experiment [15]
$m=1, n=3$	0.120	0.120	0.119	0.123
$m=1, n=4$	0.074	0.073	0.073	0.076
$m=2, n=5$	0.179	0.177	0.175	0.180
$m=2, n=6$	0.135	0.134	0.133	0.137
$m=3, n=8$	0.181	0.178	0.177	0.176
$m=3, n=9$	0.170	0.166	0.166	0.165

Table 2: Fluid-filled shell's frequencies (Hz)

Mode number	Boundary Conditions and semi-vertex angle		Ref. [13]	Ref. [3]	Present
$m=1, n=2$	C-C	$\alpha = 30^o$	79.603	79.740	80.775
		$\alpha = 60^o$	23.181	22.620	23.158
$m=1, n=3$	C-C	$\alpha = 30^o$	74.244	74.580	73.901
		$\alpha = 60^o$	22.015	21.770	22.635
$m=1, n=2$	S-S	$\alpha = 30^o$	77.139	77.560	79.832
		$\alpha = 60^o$	21.352	21.830	22.332
$m=1, n=3$	S-S	$\alpha = 30^o$	67.852	69.520	68.483
		$\alpha = 60^o$	15.396	15.470	16.269
$m=1, n=2$	C-F	$\alpha = 30^o$	23.243	23.580	24.556
		$\alpha = 60^o$	0.736	0.580	0.741
$m=1, n=3$	C-F	$\alpha = 30^o$	16.310	16.740	17.596
		$\alpha = 60^o$	0.531	0.470	0.546

Table 2 lists the natural frequencies of a fluid filled conical shell. The results of the present model are compared with those of other theories [3 and 13]. This comparison was performed for various boundary conditions and semi-vertex angles. In this example: $\frac{l}{a} = 1.0438$ and $\frac{a}{h} = 584$, where a is the middle radius of the conical shell, and $h = 1.5mm$. The natural frequencies of fluid-filled conical shells, for different circumferential mode numbers and semi-vertex angle, are plotted in

Fig.3 and compared with results available in [13]. The shell geometries used in this example include $\frac{l}{a_o}$=1.0438, $\frac{a_o}{h}$=584, *and* h=1.5*mm*. This figure shows the results are in a good agreement with those of other theories.

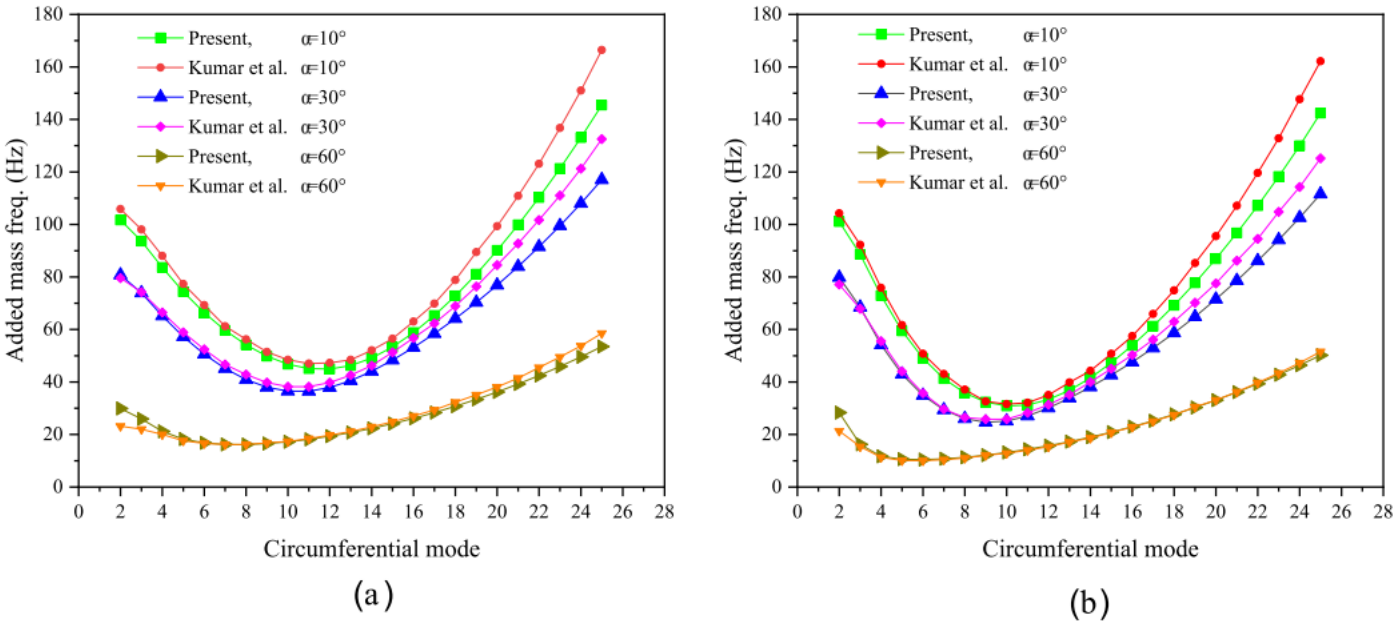

Fig. 3: Frequencies (Hz) of a conical shell (Kumar and Ganesan, [13]) for different semi-vertex angles (α = 10◦ , 30◦ , 60◦), with l/a = 1.0438, a/t = 584, and thickness 1.5 mm, (a) C–C; (b) FS-FS.

Tables 3-4 list the critical flow discharge and dimensionless frequencies for a conical shell conveying fluid with and without ring-stiffeners. Based on the critical flow discharge data presented in these tables, it is evident that the critical flow discharge increases for each successive buckling circumferential mode in comparison to an unstiffened shell. Additionally, the dimensionless frequency of a fluid-filled stiffened shell is observed to be higher than that of an unstiffened shell due to the increased stiffness of the ring stiffeners for all distinct types of boundary conditions.

Table 3: Critical flow discharge and dimensionless frequency – CC Boundary Conditions and $\alpha = 30^o$

Mode number	Critical flow discharge [m^3/s]		Dimensionless frequency	
	Stiffened	Unstiffened [13]	Stiffened	Unstiffened [13]
$m = 1, n = 7$	266	165	9.903	3.427
$m = 1, n = 8$	283	147	12.232	3.107
$m = 2, n = 9$	307	135	14.851	2.886
$m = 2, n = 10$	334	129	17.687	2.773

Table 4: Critical flow discharge and dimensionless frequency – SS Boundary Conditions and $\alpha = 30^o$

Mode number	Critical flow discharge [m^3/s]		Dimensionless frequency	
	Stiffened	Unstiffened [13]	Stiffened	Unstiffened [13]
$m = 1, n = 7$	114	110	9.068	2.231
$m = 1, n = 8$	119	98	11.315	1.976
$m = 2, n = 9$	126	90	13.904	1.872
$m = 2, n = 10$	132	94	16.563	1.906

4. Conclusion

The present model employs a hybrid finite element to predict the dynamic behaviour and buckling analysis of ring stiffened conical shells conveying fluid flow. An investigation into the geometric parameters including boundary conditions and the number of rings yields the following insights: (a) stiffeners induce higher frequencies compared to unstiffened shells, highlighting the significance of stiffener configuration on dynamic characteristics of these structures; (b) a higher number of rings increases the dimensionless frequency for fluid-filled conical shell; (c) the effect of the semi-vertex angle on the frequency response is evident, with an increase in the vertex angle leading to a decrease in flow discharge and a decrease in the dimensionless frequency of fluid-filled shells. The developed mathematical model is applicable to both cylindrical and conical shells made from isotropic and laminated composite materials.

References

[1] A. A. Lakis, P. Van Dyke, and H. Ouriche, "Dynamic analysis of anisotropic fluid-filled conical shells," *J. of Fluids and Structures*, vol. 6, no. 2, pp. 135-162, 1992.

[2] Y. Kerboua, A. A. Lakis, and M. Hamila, "Vibration analysis of truncated conical shells subjected to flowing fluid," *Applied Mathematical Modelling*, vol. 34, no. 3, pp. 791-809, 2010.

[3] M. Rahmanian, R. D. Firouz-Abadi, and E. Cigeroglu, "Free vibrations of moderately thick truncated conical shells filled with quiescent fluid," *Journal of Fluids and Structures*, vol. 63, pp. 280–301, 2016.

[4] M. Rahmanian, R. D. Firouz-Abadi, and E. Cigeroglu, "Dynamics and stability of conical/cylindrical shells conveying subsonic compressible fluid flows with general boundary conditions," *International Journal of Mechanical Sciences*, vol. 120, pp. 42–61, 2017.

[5] M. Chen, C. Zhang, X. Tao, and N. Deng, "Structural and acoustic responses of a submerged stiffened conical shell," *Shock and Vibration*, 2014.

[6] M. Liu, J. Liu, and Y. Cheng, "Free vibration of a fluid loaded ring-stiffened conical shell with variable thickness," *Journal of Vibration and Acoustics*, vol. 136, no. 5, pp. 1-10, 2014.

[7] S. M. Banijamali and A. A. Jafari, "Free vibration analysis of rotating functionally graded conical shells reinforced by anisogrid lattice structure," *Mechanics Based Design of Structures and Machines*, vol. 51, no. 4, pp. 1881–1903, 2023.

[8] K. Xie, M. Chen, L. Zhang, W. Li, and W. Dong, "A unified semi-analytic method for vibro-acoustic analysis of submerged shells of revolution," *Journal of Ocean Engineering*, vol. 189, 106345, 2019.

[9] C. Zhang, G. Jin, Z. Wang, and Y. Sun, "Dynamic stiffness formulation and vibration analysis of coupled conical-ribbed cylindrical-conical shell structure with general boundary condition," *Journal of Ocean Engineering*, vol. 234, 109294, 2021.

[10] J. Wu and Y. Sun, "An exact solution for vibration analysis of pipe coupled with conical ring stiffened cylindrical shells with arbitrary boundary condition," *Journal of Ocean Engineering*, vol. 266, 112861, 2022.

[11] A. Saboo and M. Kumar, "Dynamic analysis of partially filled cylindrical-conical-cylindrical shell representing a pressure vessel," *Journal of Thin-Walled Structures*, vol. 183, 110342, 2023.

[12] M. Zarei, G. Rahimi, and M. Hemmatnezhad, "Free vibration characteristics of grid-stiffened truncated composite conical shells," Aerospace and Technology, vol. 99, 105717, 2020.

[13] D. S. Kumar and N. Ganesan, "Dynamic analysis of conical shells conveying fluid," Journal of Sound and Vibration, vol. 310, no. 1-2, pp.38-57, 2008.

[14] M. Esmaeilzadehazimi, M. Bakhtiari, M. Toorani, and A. A. Lakis, "Numerical modeling and analysis of fluid-filled truncated conical shells with ring stiffeners," Journal of Fluids and Structures, vol. 127, 104121, 2024.

[15] U. S. Lindholm and WCL Hu, "Non-symmetric transverse vibrations of truncated conical shells," *International Journal of Mechanical Sciences*, vol. 8, no. 9, pp. 561–579, 1966.